SUBATECH

Laboratoire de physique subatomique et des technologies associées

Unité Mixte de Recherche 6457
Ecole des Mines de Nantes, IN2P3/CNRS, Université de Nantes

HALF-LIVES OF LIGHT NUCLEUS EMISSION BELOW THE BARRIER

C Bonilla and G Royer

Rapport Interne SUBATECH 2002 / 03

Adresse : Subatech - Ecole des Mines de Nantes

Half-lives of light nucleus emission below the barrier

C Bonilla, G Royer

Laboratoire Subatech, UMR: IN2P3/CNRS-Université-Ecole des Mines,
4 rue A. Kastler, 44307 Nantes Cedex 03, France
E-mail : royer@subatech.in2p3.fr

Abstract. The Be, Li, He, and H decay half-lives of slightly excited nuclei have been determined within a tunneling process through a potential barrier calculated from a generalized liquid drop model and quasi-molecular shapes. Analytic formulae allowing to obtain rapidly these different partial half-lives are proposed. For a given decay they depend only on the mass and charge numbers of the emitter, the Q value and the excitation energy.

PACS numbers: 25.85.Ec; 25.85.-w; 21.10.Tg

1. Introduction

The transmutation of nuclear waste and the production of energy and radio-isotopes by accelerator-driven systems is under consideration [1]. Within these projects, the interaction of the nucleon beam with the target, often lead or lead-bismuth mixture, induces the formation of an excited system and, besides neutrons and fission fragments [2], other reaction products are formed through different reaction mechanisms. The knowledge of all the nuclear reactions which constitute a non negligible part of the reaction cross section is needed. The energy range is from thermal up to a GeV.

In this work the study of a specific decay channel is presented: the light nucleus emission from a mother nucleus having an excitation energy lower than the decay barrier height. More precisely, the Be, Li, He, and H decay half-lives of excited nuclei in the lowest part of the intermediate-energy domain have been determined within a tunneling process through a potential barrier calculated from a generalized liquid drop model and quasimolecular shapes. Finally, analytic formulae allowing to determine rapidly these different partial half-lives are proposed. For a fixed decay they depend only on the charge and mass numbers of the excited nucleus, the Q value and the excitation energy.

2. Quasi-molecular shapes

To describe the very light nucleus emission till the rupture of the matter bridge between the emitted particle and the daughter nucleus, the quasimolecular shape sequence previously used to describe the fusion [3], fission [4, 5], cluster radioactivity [6, 7] and the α emission [8] has been kept (see Fig. 1). It allows to reproduce the formation of a deep neck while keeping spherical ends and to reach rapidly the configuration of two touching spheres. Mathematically, the shapes are two half-lemniscatoids joined on a plane perpendicular to the emission axis. At the separation point the distance between the mass centres are very small and the main part of this exit channel corresponds to two separated spherical nuclei. Consequently, the selected one-body shape plays a minor role in determining the potential barrier.

3. Potential barriers

The potential energy is calculated within the generalized liquid drop model previously defined and used to describe the less asymmetric different exit channels [9].
The macroscopic energy is given by

$$E = E_V + E_S + E_C + E_N. \tag{1}$$

For the one-body shapes at the beginning of the decay process, the volume E_V, surface E_S and Coulomb E_C energies are defined as:

$$E_V = -15.494(1 - 1.8I^2)A \ MeV, \tag{2}$$

$$E_S = 17.9439(1 - 2.6I^2)A^{2/3}(S/4\pi R_0^2) \ MeV, \tag{3}$$

$$E_C = 0.6e^2(Z^2/R_0) \times 0.5 \int (V(\theta)/V_0)(R(\theta)/R_0)^3 \sin\theta d\theta. \tag{4}$$

$I = (A_1 - A_2)/A$ and S are the relative neutron excess and the surface of the one-body deformed nucleus. $V(\theta)$ is the electrostatic potential on the surface, reducing to V_0 for the sphere.
When the light particle and daughter nucleus are separated and spherical:

$$E_{V12} = -15.494 \left[(1 - 1.8I_1^2)A_1 + (1 - 1.8I_2^2)A_2\right] \ MeV, \tag{5}$$

$$E_{S12} = 17.9439 \left[(1 - 2.6I_1^2)A_1^{2/3} + (1 - 2.6I_2^2)A_2^{2/3}\right] \ MeV, \tag{6}$$

$$E_{C12} = 0.6e^2 Z_1^2/R_1 + 0.6e^2 Z_2^2/R_2 + e^2 Z_1 Z_2/r, \tag{7}$$

where $A_i (i = 1, 2)$,Z_i,R_i and I_i are respectively the mass, charge, radius and relative neutron excess of the two nuclei. r is the distance between the mass centres.
The radius R_0 of the excited decaying nucleus is defined by

$$R_0 = (1.28A^{1/3} - 0.76 + 0.8A^{-1/3}) \ fm. \tag{8}$$

This later formula, often used only to calculate the proximity energy, allows to better reproduce the experimentally observed increase of the ratio $r_0 = R/A^{1/3}$ with the mass; for example, $r_0 = 1.10fm$ for ^9Be and $r_0 = 1.175fm$ for ^{208}Pb. In contrast, in the RLDM and RFRM approaches [10, 11] the reduced radius r_0 is chosen as $1.225fm$ and $1.16fm$ assuming no mass dependence while the surface coefficient a_s takes on the values $17.94MeV$ and $21.13MeV$. The radii of the two emitting nuclei are determined assuming volume conservation and respecting the mass ratio between the two nuclei [8]. The surface energy term E_S results from the surface tension force effects in a half space. It does not include the effects of the attractive nuclear forces between the surfaces in regard in the neck or the gap between the nascent or formed fragments. The nuclear proximity energy term E_N allows to take into account these additional surface effects when a neck or a gap appears. This term is crucial to describe correctly the one-body to two-body transition. For example, at the contact point between two spherical ^3H and ^{206}Tl nuclei the proximity energy reaches $-10MeV$.

$$E_N(r) = 2\gamma \int_{h_{min}}^{h_{max}} \Phi\left[D(r,h)/b\right] 2\pi h dh. \tag{9}$$

h is the transverse distance varying from the neck radius or zero to the height of the neck border. D is the distance between the opposite surfaces in regard and the surface width b is fixed at $0.99fm$. Φ is the proximity function of Feldmeier [12]. γ is the surface parameter given by the geometric mean between the surface parameters of the two nascent nuclei:

$$\gamma = 0.9517\sqrt{(1-2.6I_1^2)(1-2.6I_2^2)}\ MeV fm^{-2}. \tag{10}$$

In this GLDM the surface diffuseness is not taken into account and the proximity energy vanishes when there is no neck as for an alone ellipsoid for example.

To determine the half-lives the experimental decay Q value which incorporates all the microscopic corrections must be reproduced accurately. It has been introduced to improve the barrier profile in adding the difference between the experimental Q value and the theoretical one given by the GLDM at the macroscopic potential energy of the mother nucleus with an attenuation factor linear in r and vanishing at the contact point between the two spherical nascent nuclei.

As an example the potential barrier governing the ^3H decay from a ^{209}Pb nucleus (formed in the reaction $n +^{208} Pb$) is displayed in figure 2. The nuclear proximity energy smoothes strongly the completely unrealistic pure Coulomb peak, the maximum of which corresponding to the contact point between the two spheres. The barrier height is lowered by $3.7MeV$ and the peak is shifted of $2.5fm$ towards a more external position corresponding to two separated spheres maintained in unstable equilibrium by the balance between the repulsive Coulomb forces and the attractive nuclear proximity forces. The minor role played by the one-body shapes in the decay is clearly pointed

out.

4. Half-lives of light nucleus emission

In this work only the light nucleus decay from nuclei with an excitation energy E^* below the potential barrier height is considered. Then the decay can be viewed as a tunneling process and within a very asymmetric fission for which the preformation probability at the surface is one. Consequently the decay constant of the light nucleus emission is simply given by

$$\lambda = \nu_0 P. \tag{11}$$

The assault frequency ν_0 has been taken as

$$\nu_0 = 10^{20}\ s^{-1}. \tag{12}$$

The barrier penetrability P is calculated within the action integral

$$P = exp[-\frac{2}{\hbar}\int_{r_{in}}^{r_{out}} \sqrt{2B(r)(E(r) - E^*)}dr], \tag{13}$$

where r_{in} and r_{out} correspond to the points where $E(r) = E^*$ (see Fig. 3).
The inertia B(r) is related to the reduced mass by [7]

$$B(r) = \mu(1 + 1.3f(r)) \tag{14}$$

with

$$f(r) = \begin{cases} \sqrt{\frac{R_{cont}-r}{R_{cont}-R_{in}}}, r \leq R_{cont} \\ 0, r \geq R_{cont} \end{cases} \tag{15}$$

The partial half-life is finally obtained by

$$T_{1/2} = \frac{ln2}{\lambda}. \tag{16}$$

In preceding works [6, 7, 8] it has been shown that these procedures for determining the potential barriers and the partial half-lives allow to reproduce accurately the α and cluster emission half-lives. This can be observed also in figure 4 particularly devoted to heavy nuclides.

5. Analytical formulae for the α decay half-lives

For the α decay of a non excited nucleus several expressions have been proposed [13, 14] for $Log_{10}\left[T_{1/2}(s)\right]$ since the Geiger and Nutall plots [15]. Previously [8], a fitting procedure on experimental data for 373 α emitters having an α branching ratio close to one has led to the following formulas respectively for the even Z-even N, even-odd.

odd-even and odd-odd nuclei . A and Z are the mass and charge of the mother nucleus. The rms deviation is respectively 0.285, 0.39, 0.36 and 0.35.

$$log_{10}\left[T_{1/2}(s)\right] = -25.31 - 1.1629A^{1/6}\sqrt{Z} + \frac{1.5864Z}{\sqrt{Q_\alpha}}, \tag{17}$$

$$log_{10}\left[T_{1/2}(s)\right] = -26.65 - 1.0859A^{1/6}\sqrt{Z} + \frac{1.5848Z}{\sqrt{Q_\alpha}}, \tag{18}$$

$$log_{10}\left[T_{1/2}(s)\right] = -25.68 - 1.1423A^{1/6}\sqrt{Z} + \frac{1.592Z}{\sqrt{Q_\alpha}}, \tag{19}$$

$$log_{10}\left[T_{1/2}(s)\right] = -29.48 - 1.113A^{1/6}\sqrt{Z} + \frac{1.6971Z}{\sqrt{Q_\alpha}}. \tag{20}$$

Here, to take into account the excitation energy of the mother nucleus the following form has been assumed

$$log_{10}\left[T_{1/2}(s)\right] = (a_1 + a_2A^{\frac{1}{6}}\sqrt{Z} + a_3\frac{Z}{\sqrt{Q+E^*}})(1 + b_1E^* + b_2\,E^{*2}). \tag{21}$$

The coefficients have been determined from a whole set of theoretical data given by the GLDM, the experimental data being absent.

For the even Z- even N nuclei the following formula has been obtained with a rms deviation of 0.28 between the data set given by the GLDM and the values given by the formula

$$log_{10}\left[T_{1/2}(s)\right] = (-25.31 - 1.1629A^{\frac{1}{6}}\sqrt{Z} + \frac{1.5864\,Z}{\sqrt{Q_\alpha + E^*}})$$
$$\times(1 - 4.5182 \times 10^{-4}\,E^{*2}). \tag{22}$$

For the even-odd the relation (23) leads to a rms deviation of 0.41

$$log_{10}\left[T_{1/2}(s)\right] = (-26.65 - 1.0859A^{\frac{1}{6}}\sqrt{Z} + \frac{1.5848\,Z}{\sqrt{Q_\alpha + E^*}})$$
$$\times(1 + 1.1170 \times 10^{-2}\,E^* - 1.4903 \times 10^{-3}\,E^{*2}). \tag{23}$$

For the odd-even nuclei the rms deviation is 0.27

$$log_{10}\left[T_{1/2}(s)\right] = (-25.68 - 1.1423A^{\frac{1}{6}}\sqrt{Z} + \frac{1.592\,Z}{\sqrt{Q_\alpha + E^*}})$$
$$\times(1 + 8.9617 \times 10^{-3}\,E^* - 1.3446 \times 10^{-3}\,E^{*2}). \tag{24}$$

For the odd-odd nuclei the following formula leads to a rms deviation of 0.5

$$log_{10}\left[T_{1/2}(s)\right] = (-29.48 - 1.113A^{\frac{1}{6}}\sqrt{Z} + \frac{1.6971\,Z}{\sqrt{Q_\alpha + E^*}})$$
$$\times(1 - 8.8806 \times 10^{-3}\,E^*). \tag{25}$$

The introduction of the excitation energy does not diminish the accuracy of the formulae.

6. Analytical formulae for the Be, Li, He, and H decay half-lives

For excitation energies below the potential barrier height the above-mentioned procedure has been applied for the Be, Li, He, and H decay half-lives.

For ${}^{9}_{4}Be$ the formula is, with a rms deviation of 0.48,

$$log_{10}\left[T_{1/2}(s)\right] = (-31.69 - 2.238A^{\frac{1}{6}}\sqrt{Z} + \frac{4.47183\,Z}{\sqrt{Q+E^*}})$$
$$\times(1 + 2.384 \times 10^{-3}\,E^* - 9.556 \times 10^{-5}\,E^{*2}). \quad (26)$$

For ${}^{7}_{3}Li$, with $\sigma = 0.38$,

$$log_{10}\left[T_{1/2}(s)\right] = (-27.55 - 1.796A^{\frac{1}{6}}\sqrt{Z} + \frac{3.0016\,Z}{\sqrt{Q+E^*}})$$
$$\times(1 + 2.665 \times 10^{-3}\,E^* - 1.109 \times 10^{-4}\,E^{*2}). \quad (27)$$

For ${}^{6}_{3}Li$, with $\sigma = 0.36$,

$$log_{10}\left[T_{1/2}(s)\right] = (-27.45 - 1.647A^{\frac{1}{6}}\sqrt{Z} + \frac{2.8051Z}{\sqrt{Q+E^*}})$$
$$\times(1 + 3.107 \times 10^{-3}\,E^* - 1.213 \times 10^{-4}\,E^{*2}). \quad (28)$$

For ${}^{6}_{2}He$, with $\sigma = 0.35$,

$$log_{10}\left[T_{1/2}(s)\right] = (-24.85 - 1.424A^{\frac{1}{6}}\sqrt{Z} + \frac{1.8773Z}{\sqrt{Q+E^*}})$$
$$\times(1 + 2.873 \times 10^{-3}\,E^* - 1.288 \times 10^{-4}\,E^{*2}). \quad (29)$$

For ${}^{3}_{2}He$, with $\sigma = 0.24$,

$$log_{10}\left[T_{1/2}(s)\right] = (-23.60 - 1.003A^{\frac{1}{6}}\sqrt{Z} + \frac{1.3665Z}{\sqrt{Q+E^*}})$$
$$\times(1 + 3.896 \times 10^{-3}\,E^* - 1.662 \times 10^{-4}\,E^{*2}). \quad (30)$$

For ${}^{3}_{1}H$, with $\sigma = 0.14$,

$$log_{10}\left[T_{1/2}(s)\right] = (-22.65 - 0.7187A^{\frac{1}{6}}\sqrt{Z} + \frac{0.6775Z}{\sqrt{Q+E^*}})$$
$$\times(1 + 3.079 \times 10^{-3}\,E^* - 1.795 \times 10^{-4}\,E^{*2}). \quad (31)$$

For ${}^{2}_{1}H$, with $\sigma = 0.16$,

$$log_{10}\left[T_{1/2}(s)\right] = (-22.02 - 0.6039A^{\frac{1}{6}}\sqrt{Z} + \frac{0.5626Z}{\sqrt{Q+E^*}})$$
$$\times(1 + 3.06 \times 10^{-3}\,E^* - 1.871 \times 10^{-4}\,E^{*2}). \quad (32)$$

For ${}^{1}_{1}H$, with $\sigma = 0.08$,

$$log_{10}\left[T_{1/2}(s)\right] = (-21.32 - 0.4214A^{\frac{1}{6}}\sqrt{Z} + \frac{0.3961Z}{\sqrt{Q+E^*}})$$
$$\times(1 + 1.208 \times 10^{-3}\,E^* - 9.972 \times 10^{-5}\,E^{*2}). \quad (33)$$

In the case of the proton the relative neutron excess I_2 has been fixed to 1/3 in the GLDM. The partial half-lives are almost insensitive to the selected value.

It is interesting to observe that the rms deviation remains low even for the highest asymmetries. As an example, the dependence of the partial half-lives on the emitted light nucleus and the excitation energy is shown in Fig. 5 for a ^{209}Pb nucleus formed and excited by the absorption of one neutron. The Q value is positive only for the α emission. For the ^{209}Pb nucleus, the potential barrier heights are respectively $39.9 MeV$ for the ^{9}Be emission, 36.8 for ^{7}Li, 37.6 for ^{6}Li, 29.2 for ^{6}He, 32.0 for ^{3}He, 20.2 for ^{3}H, 19.7 for ^{2}H and 18.6 MeV for ^{1}H emission.

7. Summary and conclusion

The Be, Li, He, and H decay half-lives of nuclei have been determined to contribute to improve our knowledge of the decay of moderately excited nuclei. Such processses might particularly appear in accelerator driven systems. The decay has been studied for excitation energy lower than the potential barrier height and as a tunneling process through a potential barrier calculated from quasimolecular shapes and a generalized liquid drop model taking into account both the proximity energy and the asymmetry. No new parameter has been introduced in this model previously defined and used to describe the fusion, fission and cluster and α emissions.

Analytic formulae allowing to determine rapidly these different partial half-lives are proposed. For a given decay they depend only on the mass and charge numbers of the emitter, the Q value and the excitation energy.

References

[1] Rubbia C, Rubio J A, Buono S, Carminati F, Fletier N, Galvez J, Geles C, Kadi Y, Klapisch R, Mandrillon P, Revol J P and Roche Ch 1995 *CERN Report* CERNAT95-44 (ET).

[2] Duijvestijn M C, Koning A J and Hambsch F J 2001 *Phys. Rev.* C **64** 014607.

[3] Royer G and Remaud B 1985 *Nucl. Phys.* A **444** 477.

[4] Royer G and Remaud B 1984 *J. Phys.* G **10** 1057.

[5] Royer G and Haddad F 1995 *Phys. Rev* C **51** 2813.

[6] Royer G, Gupta R K and Denisov V Y 1998 *Nucl. Phys.* A **632** 275.

[7] Royer G and Moustabchir R. 2001 *Nucl. Phys.* A **683** 182.

[8] Royer G 2000 *J. Phys.* G **26** 1149.

[9] Royer G 1999 *Heavy Elements and Related New Phenomena*, ed R K Gupta and W Greiner (Singapore : World Scientific) p.591.

[10] Sierk A J 1985 *Phys. Rev. Lett.* **55** 582.

[11] Sierk A J 1986 *Phys. Rev.* C **33** 2039.

[12] Feldmeier H 1979 12th *Summer School on Nuclear Physics* (Mikolajki).

[13] Viola V E and Seaborg G T 1966 *J. Inorg. Nucl. Chem.* **28** 741.
[14] Brown B A 1992 *Phys. Rev.* C **46** 811.
[15] Geiger H and Nutall J M 1911 *Philos. Mag.* **22** 613.

Figure captions

Fig. 1. Shape evolution from a sphere towards two spheres via compact quasimolecular configurations. After the separation the fragments are supposed to be spherical.

Fig. 2. Potential barrier against ^{3}H emission from a ^{209}Pb excited nucleus. The solid and dashed lines correspond respectively to the deformation energy with and without introducing a nuclear proximity energy term. r is the centre-of-mass distance.

Fig. 3. Potential barrier governing the ^{3}He emission from ^{108}Te. E^{*} is the excitation energy and r_{in} and r_{out} the turning points. r is the centre-of-mass distance.

Fig. 4. $log_{10}[T_{1/2}(s)]$ for the α emission from Th, U, Pu, Cm, Cf and Fm isotopes. The open and full circles correspond respectively to the experimental and theoretical data versus the neutron number N.

Fig. 5. $log_{10}[T_{1/2}(s)]$ as functions of the excitation energy E^{*} (MeV) and the emitted light particle for an excited ^{209}Pb nucleus.

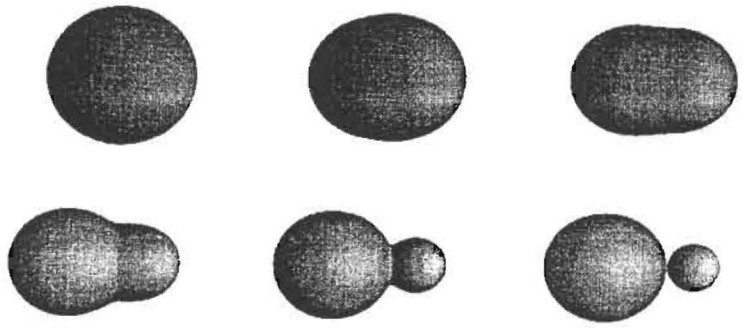

Fig. 1.

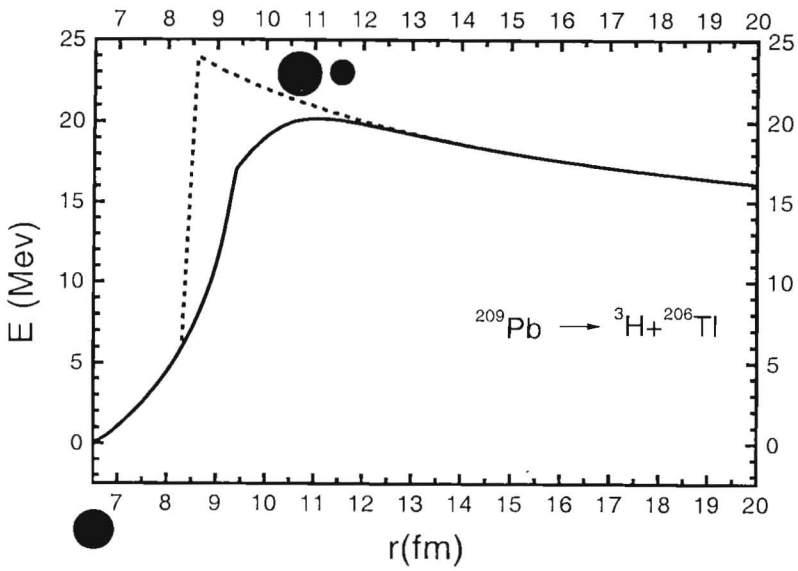

Fig. 2.

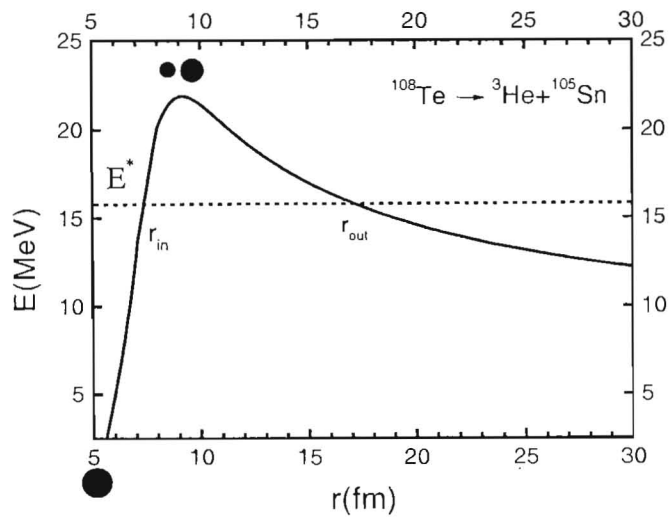
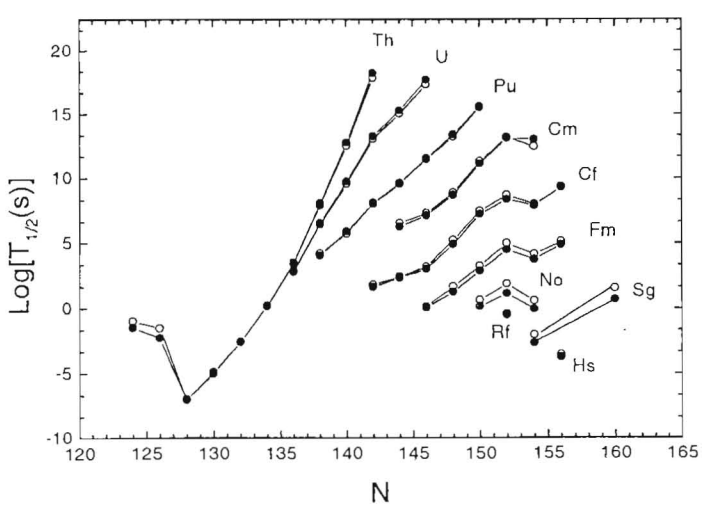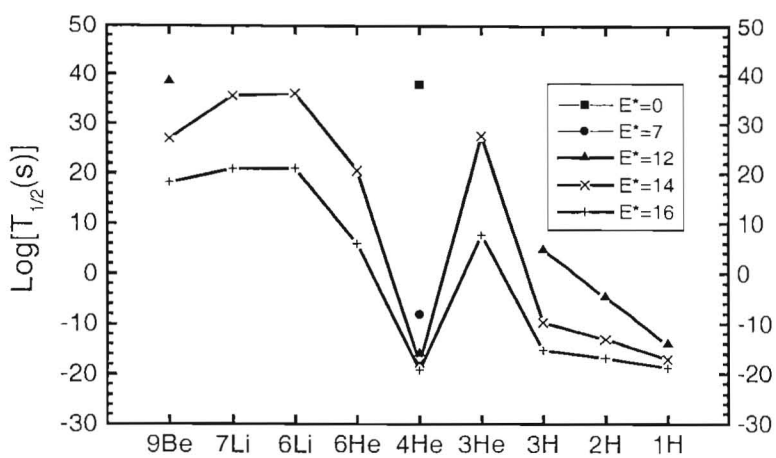
Fig. 3.